International Journal of Nanomedicine

Dovepress
open access to scientific and medical research

Open Access Full Text Article

ORIGINAL RESEARCH

Hydrophobically modified chitosan nanoliposomes for intestinal drug delivery

This article was published in the following Dove Press journal:
International Journal of Nanomedicine

M Gulrez Zariwala[1]
Harshada Bendre[2]
Anatoliy Markiv[3]
Sebastien Farnaud[4]
Derek Renshaw[4]
Kevin MG Taylor[2]
Satyanarayana Somavarapu[2]

[1]Faculty of Science and Technology, University of Westminster, London, UK; [2]Department of Pharmaceutics, University College London School of Pharmacy, London, UK; [3]Faculty of Life Sciences and Medicine, King's College London, London, UK; [4]Faculty of Health and Life Sciences, Coventry University, Coventry, UK

Background: Encapsulation of hydrophilic drugs within liposomes can be challenging.
Methods: A novel chitosan derivative, O-palmitoyl chitosan (OPC) was synthesized from chitosan and palmitoyl chloride using methane-sulfonic acid as a solvent. The success of synthesis was confirmed by Fourier transform infra-red (FT-IR) spectroscopy and proton NMR spectroscopy (H-NMR). Liposomes encapsulating ferrous sulphate as a model hydrophilic drug for intestinal delivery were prepared with or without OPC inclusion (Lipo-Fe and OPC-Lipo-Fe).
Results: Entrapment of iron was significantly higher in OPC containing liposomes compared to controls. Quantitative iron absorption from the OPC liposomes was significantly higher (1.5-fold $P<0.05$) than free ferrous sulphate controls. Qualitative uptake analysis by confocal imaging using coumarin-6 dye loaded liposomes also indicated higher cellular uptake and internalization of the OPC-containing liposomes.
Conclusion: These findings suggest that addition of OPC during liposome preparation creates robust vesicles that have improved mucoadhesive and absorption enhancing properties. The chitosan derivative OPC therefore provides a novel alternative for formulation of delivery vehicles targeting intestinal absorption.

Keywords: gut delivery, intestinal absorption, Caco-2, ferrous sulfate

Introduction

Liposomes are formed from the spontaneous reordering and organization of phospholipid molecules in an aqueous medium that results in the formation of vesicles comprising one or more lipidic bilayers and an aqueous core.[1] Bioactive molecules can either be encapsulated within the core, or incorporated within the phospholipid bilayer/bilayer interphase. Since they are composed of biologically similar lipids, liposomes are nontoxic, biocompatible, and biodegradable as a carrier system.[2] Liposomes thus represent an attractive delivery system for pharmaceutical applications where they can be utilized for targeted and controlled drug delivery, and in the cosmetic and food industry where the focus is on protection of the active ingredient and enhanced permeability and absorption.[3,4] The lipid composition of liposomes can also affect the level of incorporation of drug/substances perhaps by affecting the packaging of vesicular bilayers.[5]

Although liposomes are capable of incorporating both hydrophilic and hydrophobic drugs, encapsulation of hydrophilic molecules is most challenging, partly due to loss of drug in the external aqueous phase during liposome formulation.[6] This issue is further exacerbated in the case of ferrous iron whereby the metal iron–lipid interaction is known to have a detrimental effect on the integrity of the lipid bilayer.[7] Ferrous sulfate is a hydrophilic drug that is commonly used for iron supplementation therapy, most often via oral delivery. Its utility is severely limited by its ability to cause adverse gastrointestinal events.[8,9] Others have also reported low iron absorption

Correspondence: Satyanarayana Somavarapu
Department of Pharmaceutics, UCL School of Pharmacy, 29–39 Brunswick Square, London WC1N 1AX, UK
Tel +44 20 7753 5987
Fax +44 20 7753 5989
Email s.somavarapu@ucl.ac.uk

submit your manuscript | www.dovepress.com
Dovepress
http://dx.doi.org/10.2147/IJN.S166901

from lipid-based iron delivery products when used as oral iron supplements.[10]

The polycationic biopolymer chitosan has been explored and employed in a number of liposome systems to improve their physiochemical stability and cellular uptake characteristics.[11–15] Chitosan is a natural polysaccharide obtained by alkaline deacetylation of chitin, the major component of crustacean shells.[16] It has an excellent biocompatibility profile due to its biodegradable nature; within the body it is metabolized by a number of enzymes (eg, lysozyme, di-N-acetyl chitobiase, N-acetyl-beta-D-glucosaminidase, and chitotriosidase).[17,18] In addition, chitosan has strong mucoadhesive properties due to the presence of amine groups in its structure, which lead to electrostatic interactions with the negatively charged cell surfaces, with resultant bioadherence.[19,20] Chitosan coating onto the surface of micro or nanoparticles is therefore frequently used as a strategy to facilitate increased gastrointestinal uptake.[21,22] Surface coating of liposomes with chitosan has also been shown to improve vesicle stability. Chitosan adsorbs strongly on the vesicle surface due to interplay between its amine groups and the negatively charged phospholipid polar heads.[23] Unmodified chitosan, however, is limited in that the surface coating it forms on the liposomes is prone to rapid degradation in the gastric environment, thus affecting vesicle integrity and impairing the utility of these carriers for oral delivery applications.[7]

Chitosan is soluble only in dilute acids, which limits formulation approaches and hence its applications.[11] Several studies have sought to improve the physical and chemical characteristics of chitosan by conjugating hydrophobic or hydrophilic moieties to its structure, such as alkyl groups, poly (ε-caprolactone), and poly (ethylene glycol) (PEG).[24,25] Acylation of chitosan can be carried out at the amino (NH_2) group, the hydroxy (OH) group, or at both (N, O acyl chitosan) to obtain hydrophobic derivatives that are soluble in organic solvents such as chloroform, acetone, and dichloromethane. These chemical modifications have led to the development of novel chitosan derivatives that have further widened its drug delivery applications.

In this study, we synthesized and characterized a novel hydrophobic chitosan derivative, O-palmitoyl chitosan (OPC), and used this to formulate liposomes loaded with ferrous sulfate as a model hydrophilic drug. Cytotoxicity, as well as qualitative and quantitative drug uptake from the liposomes, was evaluated in vitro using the human intestinal cell line Caco-2.

Materials and methods

Materials

Chitosan (chitosan oligosaccharide, molecular weight: above 5k by viscosity method) was obtained from Kitto Life Co., Seoul, Korea, and egg phosphatidylcholine (egg PC) was obtained from Lipoid (Ludwigshafen, Germany). Palmitoyl chloride, ferrous sulfate, coumarin-6, cholesterol, and all other chemicals, reagents, and solvents were of analytical or cell culture grade, and purchased from Sigma-Aldrich (Gillingham, UK). Caco-2 cells were purchased from European Collection of Cell Cultures (catalog no. 09042001; ECACC, Salisbury, UK). Ferritin ELISA Kit (product code S-22) was from Ramco (ATI Atlas, Chichester, UK) and BCA Protein Assay Kit (product no. 23225) was from Pierce (Thermo Fisher Scientific, Basingstoke, UK). Cell culture media, fetal calf serum (FCS), and reagents were from Thermo Fisher Scientific. Cell Culture Plasticware was purchased from Nunc (Roskilde, Denmark) or Corning (Amsterdam, the Netherlands). All reagents used were prepared using ultrapure water (resistivity of 18.2 MΩ cm). Prior to use, all glassware and utensils were soaked in 10% HCl and rinsed with ultrapure water to remove any potential traces of residual minerals.

Methods

Synthesis of O-palmitoyl chitosan

OPC was synthesized from chitosan and palmitoyl chloride using methanesulfonic acid as a solvent in order to protect the amino groups of chitosan. Chitosan was dissolved in methanesulfonic acid at room temperature for 1 hour and palmitoyl chloride was added dropwise with continuous stirring. The molar ratio of the repeating unit of chitosan to palmitoyl chloride was 1:2. The reaction mixture was kept under stirring conditions for 5 hours, before terminating the reaction by adding crushed ice. The resultant mixture contained OPC along with residual products such as unreacted chitosan, unreacted palmitoyl chloride, and chitosan reacted with methanesulfonic acid. Methanesulfonic acid was removed using sodium bicarbonate while the other impurities were removed using dichloromethane and chloroform to extract OPC from the mixture. Organic solvents were then evaporated using a rotary evaporator (Hei-VAP Advantage Rotary Evaporator, Schwabach, Germany) and the product dialyzed against distilled water for 2–3 days using dialysis tubing of molecular weight cutoff 7,000 Da (membrane size 7,000/3, diameter 28 mm; Medicell International, London, UK). The dialyzed product was then lyophilized for 24 hours

(–40°C) using a VirTis AdVantage 2.0 bench top freeze dryer (SP Industries, Genevac, UK) to obtain pure OPC.

Polymer characterization

H-NMR spectroscopy

Proton NMR spectroscopy was performed on OPC using a Bruker 400 Ultra Shield spectrometer (Bruker, Coventry, UK). For measurements, chitosan was dissolved in deuterium oxide (D_2O) and OPC was dissolved in deuterated chloroform ($CDCl_3$), and spectra were obtained at room temperature.

Fourier transform infra-red spectroscopy

Fourier transform infra-red (FT-IR) spectra were collected at room temperature using a Perkin Elmer Spectrum 100 spectrometer (Perkin Elmer, Buckinghamshire, UK). Data were analyzed using the Perkin Elmer Spectrum Express software (Perkin Elmer).

Differential scanning calorimetry

In order to determine the thermal properties of the reactant, chitosan, and the product, OPC, differential scanning calorimetry (DSC) experiments were performed using a DSC Q2000 module (TA Instruments, New Castle, DE, USA). Samples of approximately 5 mg (accurately weighed) were loaded onto aluminum hermetic pans. The thermal properties of chitosan were studied at a scan rate of 50°C/min and OPC was studied at 10°C/min. Both the materials were heated from –20°C to 200°C–300°C under a nitrogen atmosphere.

X-ray powder diffraction

The solid state properties of chitosan and OPC were measured by powder X-ray diffraction (XRD) studies using an Oxford Diffraction Xcalibur nova T X-ray diffractometer (Agilent Technologies, Wokingham, UK), which were processed using CrysAlis Pro software (Oxford Diffraction, Oxford, UK) and scanned at a step size of 10°2-theta.

Preparation of iron-loaded liposomes

Blank and iron-loaded liposomes were prepared by the thin-film hydration method, with some modifications.[26] Egg PC (200 mg) and cholesterol (20 mg) were dissolved in a round-bottomed flask containing 5 mL chloroform. OPC (20 mg) was simultaneously dissolved in the chloroform for preparation of OPC liposomes. Organic solvent was removed using a rotary evaporator (Hei-VAP Advantage Rotary Evaporator) under reduced pressure (10 minutes, 60°C) yielding a lipid film on the walls of the flask. The lipid film was hydrated by adding a prewarmed aqueous ferrous sulfate solution dropwise and shaking the flask vigorously while maintaining at 60°C. The lipid suspension was then transferred into a glass vial and agitated gently in an ultrasonic bath for 3 minutes after which size reduction was performed using a probe sonicator (80% sonication power, 20 seconds on and off intervals). The samples were allowed to stand for 1 hour, followed by centrifugation to remove the unentrapped drug. The four liposome formulations prepared – blank liposome (Lipo-blank), iron-containing liposomes (Lipo-Fe), liposomes incorporating OPC (OPC-Lipo), and iron-containing OPC-liposomes (OPC-Lipo-Fe) – were stored in nitrogen purged glass vials at 4°C. For uptake visualization studies coumarin-6-loaded liposomes (Lipo-Cou and OPC-Lipo-Cou) were prepared using a similar methodology.

Determination of entrapment efficiency

Iron entrapment efficiency (EE) was determined as described previously.[27,28] Briefly, liposome preparations were centrifuged (13,000 rpm, 30 minutes, 4°C), and aliquots of the supernatant were collected to quantify unassociated drug. Ferrous iron levels in the solution were measured spectrophotometrically at 572 nm using the ferrozine method.[29] Coumarin-6 concentration was determined using a microplate fluorimeter (Fluostar Optima; BMG Labtech, Ortenberg, Germany) at 450 nm/505 nm (excitation/emission). The mean values of three independent readings were recorded and the results were expressed as mean±SD.

EE was calculated using the following equation:

$$\text{EE (\%)} = \frac{\text{Unbound drug in supernatant}}{\text{Total drug added}}$$

Liposome physicochemical characterization

Size analysis

Size distribution determination of the liposomes by dynamic light scattering (DLS) was carried out using the Zetasizer Nano ZS (Malvern Instruments, Malvern, UK). Prior to measurements the liposome dispersion was diluted using MQ H_2O. All measurements were performed at 25°C, and three readings were taken for each sample to calculate mean particle size and standard deviation (SD).

Zeta potential

Zeta potential of the liposome dispersions was determined by measuring their electrophoretic mobilities using the Zetasizer

Nano ZS (Malvern Instruments). Measurements were carried out in triplicate at 25°C. All samples were diluted in water (1:10) before measuring the zeta potential.

Cytotoxicity assay

The potential toxic effects of liposome formulations on Caco-2 cells were assessed by carrying out the colorimetric MTT assay, incubating Caco-2 cell monolayers with liposome formulations diluted to final iron concentrations of 20, 50, and 100 μM (and equivalent volumes of corresponding blank liposomes) in phenol red free media for 48 and 72 hours.[28,30] Following incubation, 20 μL MTT (5 mg/mL) was added to each well and the plates were incubated for a further 4 hours. Media were then carefully aspirated and cell monolayers solubilized with DMSO (100 μL/well). The purple formazan product formed was quantified by measuring the absorbance spectrophotometrically at 550 nm to give an estimate of cell viability.

Caco-2 cell iron absorption/quantitative cellular uptake

Caco-2 cells were obtained at passage 20 and used experimentally between passages 35 and 55. Stock cultures were maintained in 75 cm^2 tissue culture flasks in complete medium (DMEM – Glutamax®, pH 7.4 supplemented with 10% FCS, 1% antibiotic/antimycotic solution, and 25 mM HEPES) in an incubator at 37°C in an atmosphere of 95% air and 5% CO_2 at constant humidity. Caco-2 cell uptake experiments were carried out as described previously and lysed samples were stored for analysis.[28,30] Total ferritin concentration of cell lysates was determined using a RAMCO ferritin ELISA kit following the manufacturer's protocol with modifications.[28] The protein content of Caco-2 cells was determined using the Pierce BCA kit following the manufacturer's protocol. Ferritin concentration was standardized against total protein concentration, and ng ferritin/mg protein was considered an index of liposomal iron uptake and absorption by Caco-2 cells.

Cellular uptake visualization/qualitative cellular uptake

Qualitative cellular uptake visualization studies were carried out as described previously with modifications.[31] The Caco-2 cell uptake experiment was carried out as described in the previous section, replacing Fe-loaded liposomes with coumarin-6 liposomes (Lipo-Cou). Briefly, Caco-2 cell monolayers were washed twice with sterile Dulbecco's phosphate buffered saline (DPBS), fixed with 3% paraformaldehyde solution, and washed again twice with DPBS before cell permeabilization solution (0.5% Triton X-100 in DPBS) was added for 5 minutes. Cells were then washed again with DPBS before being incubated with a 5% BSA block solution containing RNAse A (final concentration 10 μL/mL). Cells were then incubated with Lipo-Cou and OPC-Lipo-Cou formulations diluted in DPBS at a concentration of 1 μg/mL for 2 hours at 37°C. Cell nuclei were stained with TO-PRO-3 (1 μM; Thermo Fisher Scientific) for 1 hour at room temperature. Caco-2 cells were then examined under a confocal microscope (Leica TCS SP2; Leica Microsystems, Buckinghamshire, UK). The coumarin-6 and TO-PRO-3 were investigated at 488/520 and 642/661 nm wavelengths (excitation/emission), respectively. Images were analyzed using the Leica LCS Lite software suite (Leica Microsystems).

Statistical analysis

Data are presented as mean±SD, and differences between samples were analyzed by one-way ANOVA followed by Tukey's post hoc test using the PRISM software package (Version 6; Graphpad Software Inc., San Diego, CA, USA). Results were considered significantly different if $P \leq 0.05$.

Results

The FT-IR spectra of chitosan and OPC are shown in Figure 1. The important peaks for chitosan are the broad peak from 3,200 to 3,500 cm^{-1}, signifying the free hydroxyl and amine groups of chitosan; the small peak at 2,871 cm^{-1} signifying the acyl groups; and the peak at 1,649 cm^{-1} signifying carbonyl stretching of an amide bond, suggesting acyl substitution at the amino group of chitosan. The low intensity of the peak suggests that the degree of acetylation of chitosan is low.[32] The FT-IR spectrum of OPC differs from that of chitosan. The broad peak at 3,200–3,500 cm^{-1} is much reduced in OPC signifying substitution of the hydroxyl and amino groups of chitosan. There are two sharp peaks at 2,919 and 2,851 cm^{-1}, which signify the palmitoyl (acyl) groups, indicating acylation of chitosan. The sharp peak at 1,740 cm^{-1} signifies ester bond formation, which suggests that the substitution of the palmitoyl groups has occurred at the hydroxy groups of chitosan.[33] The peak at 1,657 cm^{-1} signifying amide bond formation is low in intensity, suggesting that the degree of N-acylation of chitosan is low.[32] These FT-IR results confirm the successful synthesis of OPC.

The proton NMR (H-NMR) spectrum of chitosan 5k (Figure 2A) shows the characteristic peaks for chitosan, which occur between 1.8 and 5.2 ppm.[33] The peak at 1.97

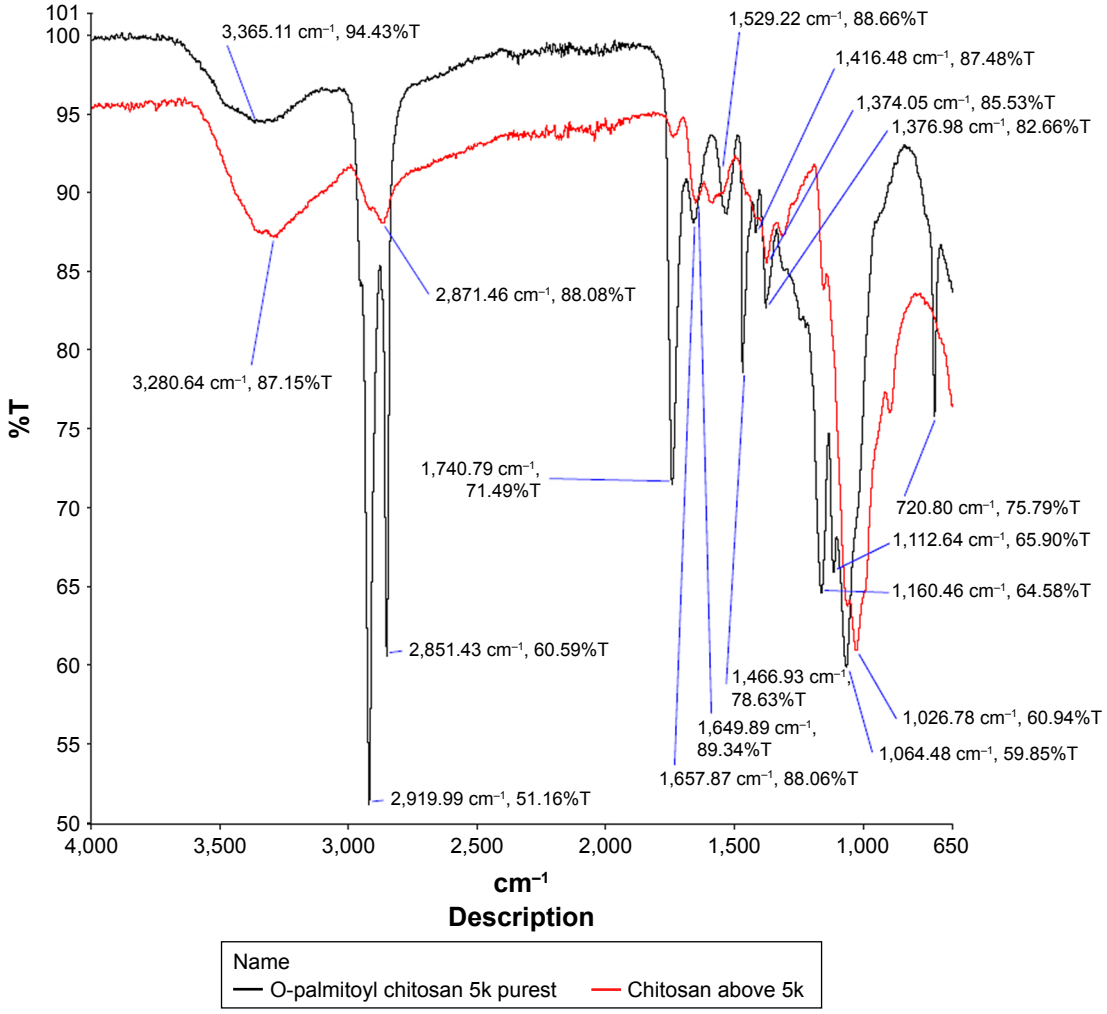

Figure 1 FT-IR spectra of chitosan 5k (red) and O-palmitoyl chitosan (black).
Abbreviations: FT-IR, Fourier transform infra-red; T, transmittance.

was assigned to the N-acetyl proton of N-acetyl glucosamine while the peak at 2.63 was assigned to a proton of N-acetyl glucosamine or glucosamine residues. The peaks from 3.3 to 4.0 ppm were assigned to the ring protons and the peaks at 4.38 and 4.40 ppm were assigned to protons of glucosamine and N-acetyl glucosamine, respectively.[32] The peak at 4.60 ppm is the D_2O solvent peak. The H-NMR spectrum of OPC (Figure 2B) differs from that of chitosan. The peaks at 0.86, 1.24, and 1.59 ppm were assigned to characteristic alkyl protons of the palmitoyl residue.[33] The peak at 0.86 ppm was assigned to the protons of the terminal carbon of the alkyl chain, that is, [CH_3-R] of the palmitoyl residue, while the peak at 1.24 ppm was assigned to the protons of the middle carbon, that is, [–CH_2–] of the alkyl chain of the palmitoyl residue. The peak at 1.59 ppm was assigned to the protons of the carbon attached to the carbonyl carbon, that is, [–(CO)–CH_2–] of the palmitoyl residue.[32] The peak at 7.24 ppm was the solvent peak for $CDCl_3$. The H-NMR data thus confirm the formation of OPC.

The DSC thermogram of chitosan (Figure 3A) showed a small endothermic peak at 70.6°C and a broad endothermic peak at 100°C–150°C which indicate loss of unbound and bound water.[34] There was also a sharp endothermic peak at 243.5°C which indicates thermal degradation of the sample.[35] The DSC thermogram of OPC (Figure 3B) did not show any thermal transitions from 0°C to 160°C. The thermogram showed a sharp endothermic peak at 182°C, indicating polymer decomposition.[36]

The X-ray diffractogram of chitosan (Figure 4A) showed peaks at 2Θ=9, 20, and 23 which were characteristics of chitosan.[32,35] The diffractogram suggested that chitosan was crystalline. The X-ray diffractogram of OPC (Figure 4B) showed a broad peak at 2Θ=21. The peaks at 2Θ=9 and 23 which were seen in chitosan have disappeared.

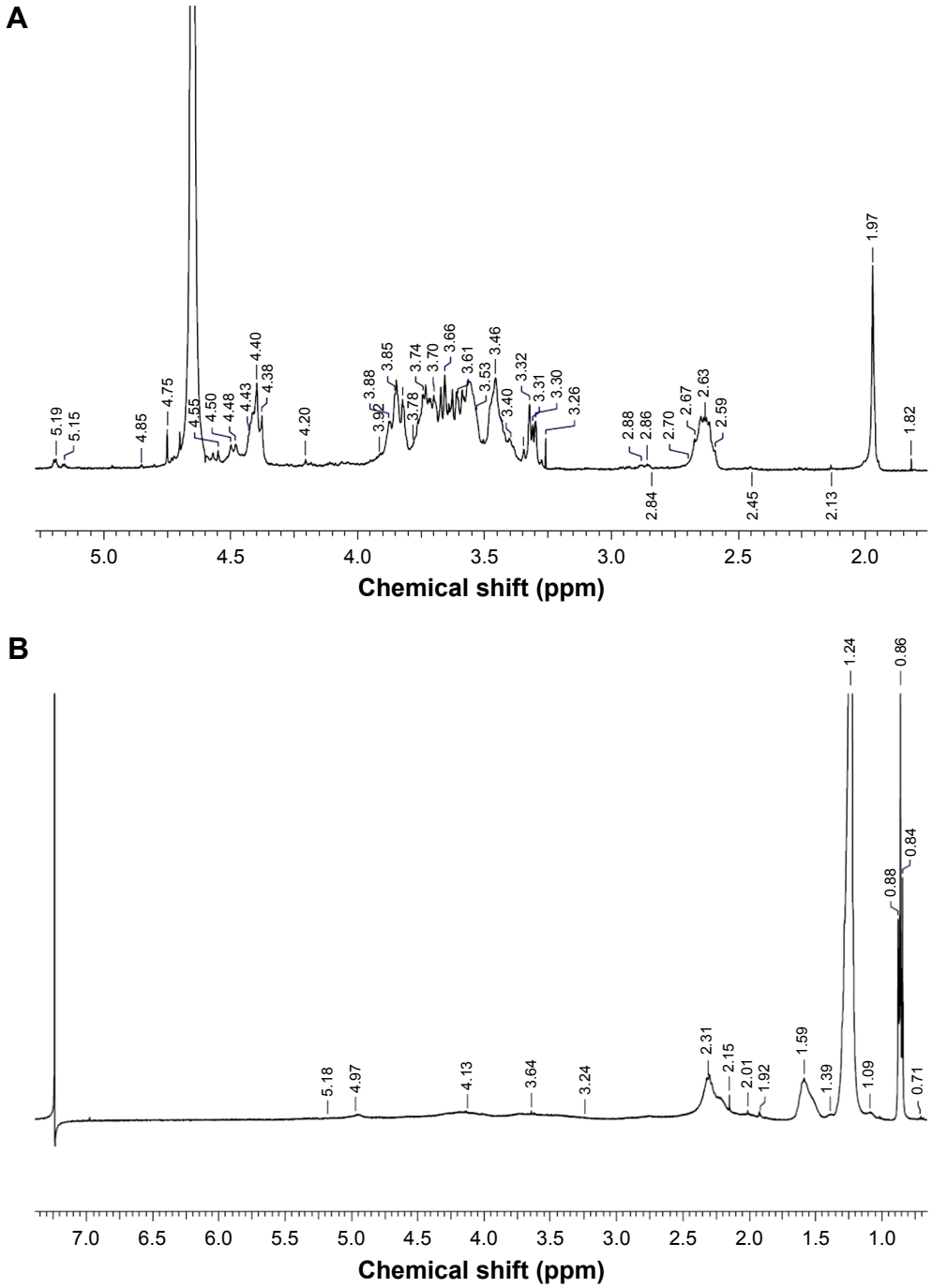

Figure 2 H-NMR spectra of (**A**) chitosan 5k and (**B**) O-palmitoyl chitosan.

The diffractogram suggested that OPC was crystalline and that o-acylation had slightly altered the chitosan structure.[35]

Both the iron-containing liposome formulations demonstrated high iron EE. The EE of Lipo-Fe was 72.8%±1.93%, which was increased and in case of OPC-Lipo-Fe, 82.7%±2.70% ($P<0.05$; Table 1). Mean hydrodynamic diameters of all liposomes were in the range 204–304 nm following sonication (Table 1). Iron loading decreased mean particle size ($P<0.05$). Chitosan imparted a positive charge to the blank and iron-loaded liposomes, confirming its presence on the outer surface of the liposomes (Table 1), whereas liposomes without OPC had a net negative zeta potential. Iron loading affected the surface charge ($P>0.05$) of OPC-containing liposomes, but decreased the negative surface charge of non-OPC liposomes ($P<0.05$), through an ionic interaction with the electric double layer.

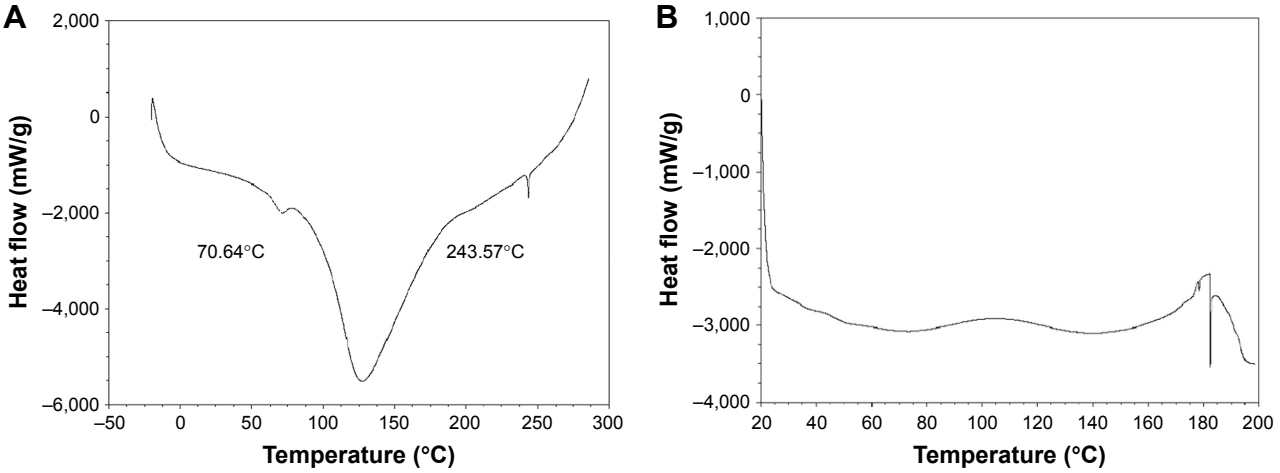

Figure 3 DSC thermogram of (**A**) chitosan (50°C/min) and (**B**) O-palmitoyl chitosan (20°C/min).
Abbreviation: DSC, differential scanning calorimetry.

Caco-2 cells were exposed to increasing concentrations of the liposome formulations standardized at specific iron concentrations (20, 50, and 100 µM elemental iron), as described previously.[28,30] Cells were also incubated with iron-free liposome formulations to exclude the effect of iron. Cell viability in all cases was observed to be at least 85% of control cells at both the experimental time points (48 and 72 hours; Figure 5).

To assess the efficacy of the liposome preparations to deliver iron intracellularly, comparative absorption experiments were conducted (Figure 6) using the well-characterized human intestinal cell line Caco-2.[37–39] Iron absorption from the liposome preparations was compared to that from free $FeSO_4$ solution, as it is generally considered to have the best bioavailability profile among iron compounds and was employed in the preparation of the liposomal formulation. The overall highest iron absorption was from OPC-Lipo-Fe liposomes (313.46±26.53 ng/mg protein) and was 1.5 fold ($P<0.05$) higher than for the free $FeSO_4$ control (200.42±24.42 ng/mg protein).

The cellular uptake characteristics of the liposome formulations were further evaluated qualitatively using confocal microscopy. Figure 7 shows confocal micrographs of Caco-2 cells incubated with conventional (Lipo-Cou) and OPC liposomes (OPC-Lipo-Cou) loaded with equivalent concentrations of the fluorescent dye coumarin-6. The results suggest that the inclusion of the OPC influenced the surface charge of the liposomes. It is likely that the OPC was incorporated into the liposome structure due to the hydrophobic nature of the chitosan.

Discussion

Several previous studies have demonstrated the use of hydrophobic chitosan derivatives for formulating drug and gene

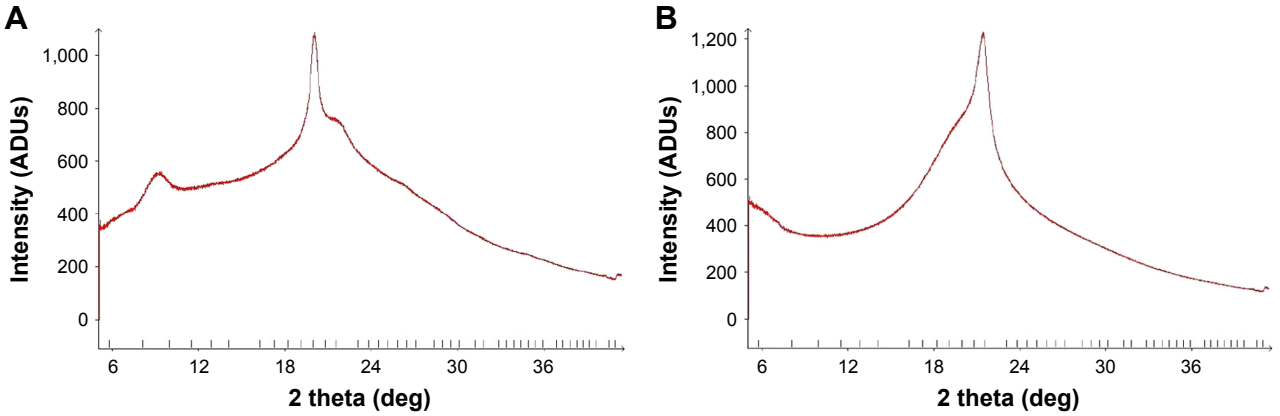

Figure 4 X-ray powder diffractograms of (**A**) chitosan and (**B**) O-palmitoyl chitosan.
Abbreviations: ADUs, analog digital units; deg, degrees.

Table 1 Particle size distribution, surface charge, and entrapment efficiencies for liposome preparations

Formulation	Mean particle size (nm)	Zeta potential (mV)	Entrapment efficiency (%)
Lipo-blank	253±17	−28.6±8.77	
Lipo-Fe	204±22	−9.82±4.33	
OPC-Lipo	304±15	33.1±6.39	72.8±1.93
OPC-Lipo-Fe	209±12	27.8±8.67	82.7±2.7

Note: Values are presented as mean±SD, n=3.
Abbreviations: Fe, iron; Lipo, liposome; OPC, octyl-palmitoyl chitosan.

delivery carriers.[40–44] In this study, a novel hydrophobically modified chitosan derivative was produced by conjugating palmitoyl to the chitosan backbone. The successful synthesis and formation of the reaction product OPC were determined by FT-IR and H-NMR, and the synthesized polymer was further characterized by DSC and XRD.

Liposomal-iron delivery has been explored previously; however, poor iron loading remains an issue. The permeability of the phospholipid bilayer of the lipid vesicles can lead to iron leakage and loss during formulation as well as upon storage. Various approaches have previously been explored to improve vesicle membrane stability. Inclusion of cholesterol in the formulation increases membrane stability, resulting in increased encapsulation efficiencies.[45–47] It is thought that the hydroxyl groups in the polar head combine with the choline groups of the lipid to create more robust bilayers.[48] Cholesterol is also known to enhance contact between adjacent lipid molecules by having a "drying" effect at the lipid–water interface, thereby decreasing bilayer permeability and promoting liposomal membrane stability.[49] PEGylated polyelectrolytes incorporation into liposomes similarly enhances drug delivery.[50] Chitosan incorporation in liposomes is known to have a positive influence on the encapsulation characteristics and delivery of liposomes.[51–53] Chitosan adsorbs at the vesicle surface due to electrostatic interactions with the lipid component thereby creating rigid walled vesicles.[54] Furthermore, chitosan reportedly forms a stable complex with iron that might also result in higher incorporation and retention in the vesicle.[55] The iron to lipid ratio is another important parameter that influences liposomal EE.[28] This study employed an iron to lipid ratio of 1:100, as increasing iron concentration has an inverse relationship with liposomal EE, an effect attributed to the strong electrolyte behavior of ferrous sulfate.[6] OPC interacts with liposomes due to positive charge and hydrophobicity, which we propose is due to the conjugation of palmitoyl groups at the O position on the chitosan structure.

We aimed to obtain liposomes in the size range obtained (approximately 200–300 nm); it has been observed previously that large-sized liposomes are more likely to be unstable and have a tendency for flocculation.[56] Furthermore, particles in the sub-500 nm range have been reported to be desirable for intestinal absorption as they facilitate increased cellular contact and permeation.[57]

The high net positive charge of the liposomes suggests electrostatic repulsion between the liposomes and is therefore considered favorable for formulation stability.[58] Positive charge on the liposome surface is also beneficial for interaction and binding with cell surfaces, potentially leading to increased cellular entry and uptake.

The absorption results obtained in our experiments are in agreement with previous in vitro and in vivo liposome studies. Hermida et al demonstrated high iron uptake in Caco-2 cells from chitosan-coated liposomes compared with

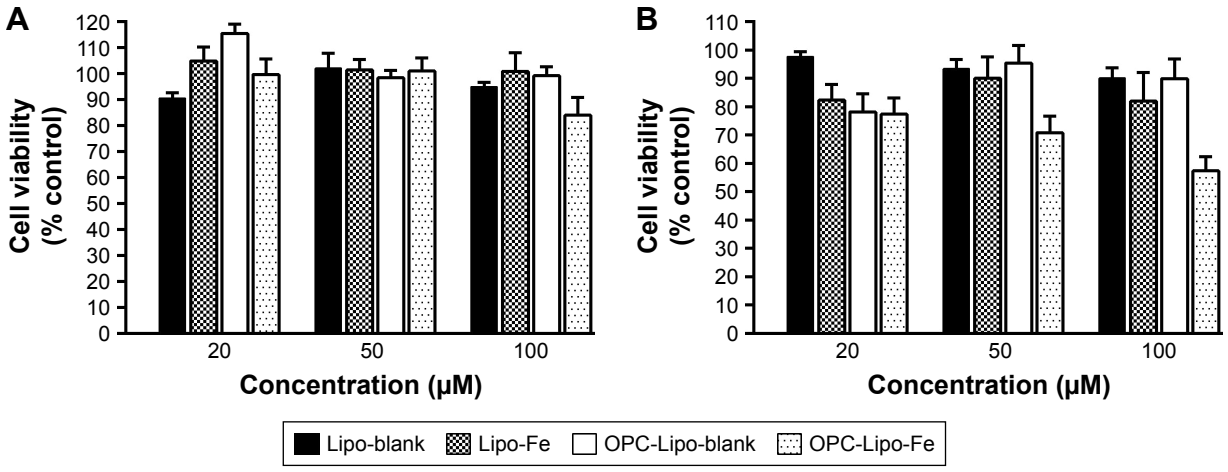

Figure 5 Caco-2 cell viability assessed by MTT assay following (**A**) 48 hours and (**B**) 72 hours incubation with liposome formulations containing increasing drug concentrations (mean±SD, n=6).

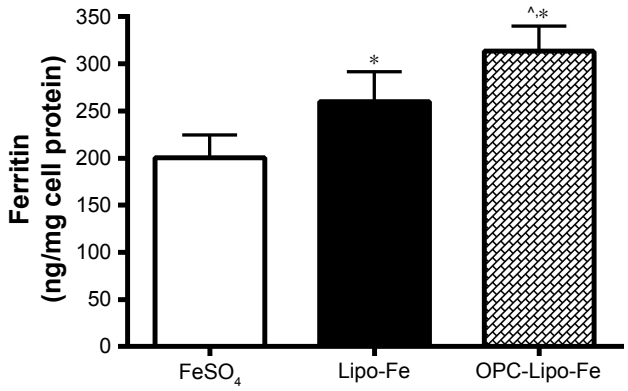

Figure 6 Iron absorption by Caco-2 cells incubated with liposome formulations: intracellular ferritin was measured as a marker of iron absorption by ELISA following 22 hours of incubation after iron uptake experiments.
Note: Results are shown as mean±SD (n=6), *Represents a significant difference (95%) between treatment and $FeSO_4$ alone. ^Represents a significant difference (95%) between OPC liposomes and liposomes alone.

uncoated liposomes.[7] The behavior of chitosan liposomes within the intestinal tract was studied by Takeuchi et al using the Wistar rat model.[59] Rat intestines were examined following administration of liposome preparations, with and without chitosan inclusion, resulting in the highest levels of retention and mucosal penetration observed with chitosan inclusion. Chitosan has well-characterized mucoadhesive properties due to its cationic structure, and also acts as a potent permeation enhancer, particularly in the pH environment encountered in the small intestine.[60]

Lipid-based carriers are known to possess high cellular permeability, presumably by virtue of ease of transport across the phospholipid bilayer of cell membranes.[61] Furthermore, the size range of our liposome particles is favorable toward intestinal absorption. The influence of particle size on intestinal absorption has been explored previously; it is generally thought that particles of 100–500 nm dimensions are most likely to diffuse through the submucosal layer and subsequently enter the cell via absorptive endocytosis.[62]

The intensity of intracellular green fluorescence emitted by coumarin-6 was considered a marker of uptake of the dye-loaded liposomes in Caco-2 cells, as described previously.[31,63] Similar studies by others have demonstrated that free coumarin-6 does not internalize in Caco-2 cells, and therefore the intracellular fluorescent intensity is a direct indicator of the internalization of the dye-loaded liposomes.[64,65] As observed in Figure 7, a green fluorescent signal was seen in both images, Figure 7B and E, indicating successful entry into the cell of coumarin-loaded liposomes; however, a noticeably stronger signal was observed in Caco-2 cells incubated with OPC-Lipo-Cou (Figure 7E)

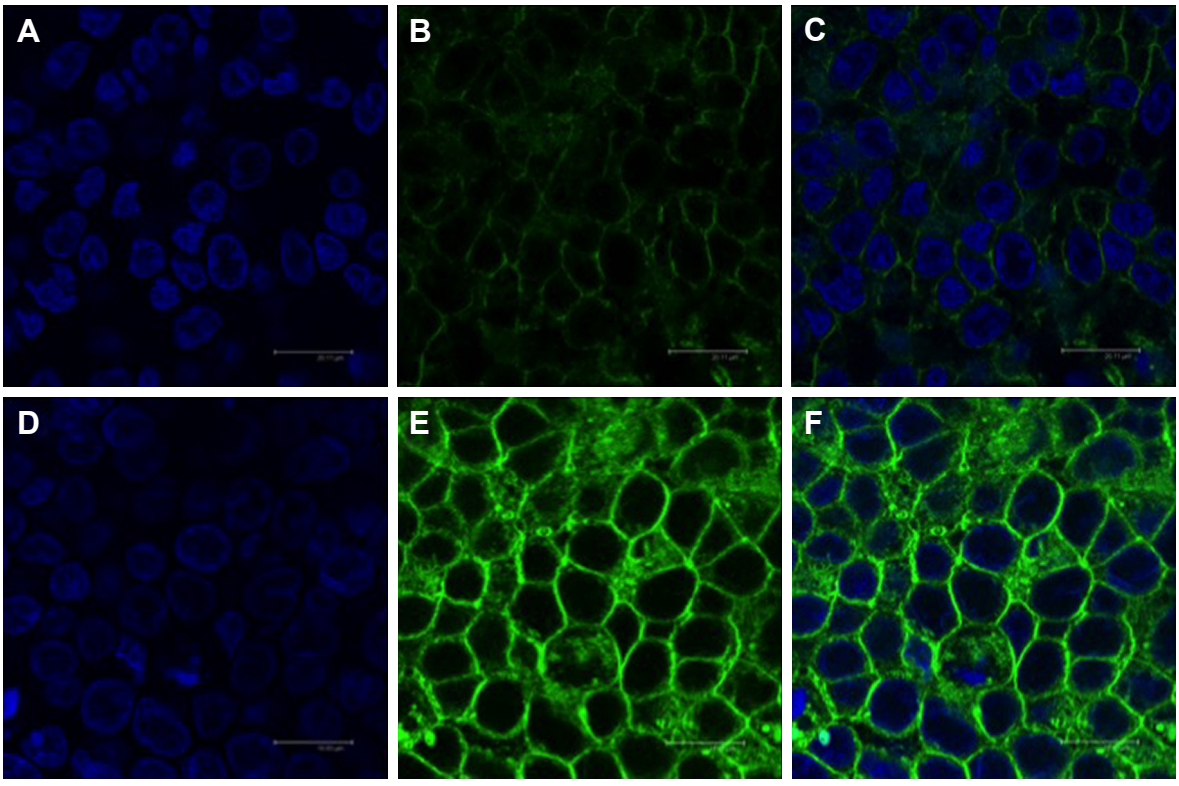

Figure 7 Confocal microscopy images of Caco-2 cells following incubation with coumarin-6 loaded (**A**–**C**) conventional (Lipo-Cou) liposomes and (**D**–**F**) OPC liposomes (OPC-Lipo-Cou).
Notes: Images (**A** and **D**) demonstrate cell nuclei stained with TO-PRO-3 (blue), images (**B** and **E**) show cell cytoplasm with accumulated liposomal coumarin-6, and images (**C** and **F**) show merged images. Scale shown is 50 μM.

compared with Lipo-Cou (Figure 7B). Confocal imaging was performed under similar parameters (sensitivity, gain, and offset) to allow an unbiased comparison. These results are in agreement with the quantitative uptake data as measured by ELISA (Figure 6), and provide further supporting evidence that OPC has a beneficial effect on the cellular uptake and internalization characteristics of the liposomes.

While mechanistic studies of the internalization and intracellular behavior of the liposomes were not conducted as part of our experiments, others have suggested potential pathways of cellular uptake and transport. Oral micro and nanoparticle drug carriers may gain cellular and subsequent systemic entry via either transcellular or paracellular pathways. Paracellular transport is thought to be limited, as the tight junctions between the intestinal enterocytes have an average pore radius of 5 nm.[66] Even under conditions of induced dilation with pharmacological agents or due to pathological insults, these junctions may allow the passage of very small-sized molecules.[67] It is speculated that lipid particles are internalized via transcytosis and endocytosis followed by physiological degradation and intracellular drug release and subsequent transport across the basolateral membrane. This model is consistent with our observations, with higher intracellular levels of coumarin-6 and ferritin protein formation observed following loaded liposome administration compared with drug alone. These results suggest that the drug released from the liposome formulations is actively processed within the enterocyte following cellular liposome uptake.

Conclusion

The purpose of this article was to synthesize a hydrophobically modified chitosan derivative and utilize this to formulate liposomes for oral drug delivery, using iron sulfate as a model hydrophilic drug. OPC not only led to increased liposomal iron encapsulation efficiency, but also significantly increased iron absorption in Caco-2 cells. These results confirm that this chitosan derivative retains the characteristic permeation-enhancing properties of chitosan, and furthermore its inclusion in the liposome may have altered the vesicle microstructure and influenced greater interaction with cell membranes leading to increased cellular uptake.

In summary, our results present OPC polymer incorporation into liposomes to be utilized for micro- and nanodelivery systems, and demonstrate the potential of OPC liposomes as promising carriers for intestinal drug delivery.

Disclosure

The authors report no conflicts of interest in this work.

References

1. Bangham AD, Standish MM, Watkins JC. Diffusion of univalent ions across the lamellae of swollen phospholipids. *J Mol Biol*. 1965;13(1):238–252.
2. Lasic DD. Novel applications of liposomes. *Trends Biotechnol*. 1998;16(7):307–321.
3. Maurer N, Fenske DB, Cullis PR. Developments in liposomal drug delivery systems. *Expert Opin Biol Ther*. 2001;1(6):923–947.
4. Taylor TM, Davidson PM, Bruce BD, Weiss J. Liposomal nanocapsules in food science and agriculture. *Crit Rev Food Sci Nutr*. 2005;45(7–8):587–605.
5. Manca ML, Sinico C, Maccioni AM, et al. Composition influence on pulmonary delivery of rifampicin liposomes. *Pharmaceutics*. 2012;4(4):590–606.
6. Xia S, Xu S. Ferrous sulfate liposomes: preparation, stability and application in fluid milk. *Food Res Int*. 2005;38(3):289–296.
7. Hermida LG, Roig A, Bregni C, Sabés-Xamaní M, Barnadas-Rodríguez R. Preparation and characterization of iron-containing liposomes: their effect on soluble iron uptake by Caco-2 cells. *J Liposome Res*. 2011;21(3):203–212.
8. Martínez-Navarrete N, Camacho MM, Martínez-Lahuerta J, Martínez-Monzó J, Fito P. Iron deficiency and iron fortified foods – a review. *Food Res Int*. 2002;35(2–3):225–231.
9. Hurrell RF. Preventing iron deficiency through food fortification. *Nutr Rev*. 1997;55(6):210–222.
10. Hartman-Craven B, Christofides A, O'Connor DL, Zlotkin S. Relative bioavailability of iron and folic acid from a new powdered supplement compared to a traditional tablet in pregnant women. *BMC Pregnancy Childbirth*. 2009;9:33.
11. Marón LB, Covas CP, da Silveira NP, et al. LUVs recovered with chitosan: a new preparation for vaccine delivery. *J Liposome Res*. 2007;17(3–4):155–163.
12. Janes KA, Calvo P, Alonso MJ. Polysaccharide colloidal particles as delivery systems for macromolecules. *Adv Drug Deliv Rev*. 2001;47(1):83–97.
13. Manca ML, Valenti D, Sales OD, et al. Fabrication of polyelectrolyte multilayered vesicles as inhalable dry powder for lung administration of rifampicin. *Int J Pharm*. 2014;472(1–2):102–109.
14. Manca ML, Peris JE, Melis V, et al. Nanoincorporation of curcumin in polymer-glycerosomes and evaluation of their in vitro–in vivo suitability as pulmonary delivery systems. *RSC Adv*. 2015;5(127):105149–105159.
15. Perugini P, Genta I, Pavanetto F, et al. Study on glycolic acid delivery by liposomes and microspheres. *Int J Pharm*. 2000;196(1):51–61.
16. Garcia-Fuentes M, Alonso MJ. Chitosan-based drug nanocarriers: where do we stand? *J Control Release*. 2012;161(2):496–504.
17. Kean T, Thanou M. Biodegradation, biodistribution and toxicity of chitosan. *Adv Drug Deliv Rev*. 2010;62(1):3–11.
18. Kumar MN, Muzzarelli RA, Muzzarelli C, Sashiwa H, Domb AJ. Chitosan chemistry and pharmaceutical perspectives. *Chem Rev*. 2004;104(12):6017–6084.
19. Filipović-Grcić J, Skalko-Basnet N, Jalsenjak I. Mucoadhesive chitosan-coated liposomes: characteristics and stability. *J Microencapsul*. 2001;18(1):3–12.
20. Sogias IA, Williams AC, Khutoryanskiy VV. Why is chitosan mucoadhesive? *Biomacromolecules*. 2008;9(7):1837–1842.
21. Garcia-Fuentes M, Torres D, Alonso MJ. New surface-modified lipid nanoparticles as delivery vehicles for salmon calcitonin. *Int J Pharm*. 2005;296(1–2):122–132.
22. Fonte P, Nogueira T, Gehm C, Ferreira D, Sarmento B. Chitosan-coated solid lipid nanoparticles enhance the oral absorption of insulin. *Drug Deliv Transl Res*. 2011;1(4):299–308.
23. Mertins O, Dimova R. Binding of chitosan to phospholipid vesicles studied with isothermal titration calorimetry. *Langmuir*. 2011;27(9):5506–5515.

24. Wang C, Li G, Tao S, Guo R, Yan Z. Crystalline and micellar properties of amphiphilic biodegradable chitooligosaccharide-graft-poly(ε-caprolactone) copolymers. *Carbohydr Polym*. 2006;64(3):466–472.
25. Yang S, Zhu J, Lu Y, Liang B, Yang C. Body distribution of camptothecin solid lipid nanoparticles after oral administration. *Pharm Res*. 1999;16(5):751–757.
26. Pupo E, Padrón A, Santana E, et al. Preparation of plasmid DNA-containing liposomes using a high-pressure homogenization – extrusion technique. *J Control Release*. 2005;104(2):379–396.
27. Ruckmani K, Sankar V. Formulation and optimization of Zidovudine niosomes. *AAPS PharmSciTech*. 2010;11(3):1119–1127.
28. Zariwala MG, Elsaid N, Jackson TL, et al. A novel approach to oral iron delivery using ferrous sulphate loaded solid lipid nanoparticles. *Int J Pharm*. 2013;456(2):400–407.
29. Stookey LL. Ferrozine – a new spectrophotometric reagent for iron. *Anal Chem*. 1970;42(7):779–781.
30. Zariwala MG, Farnaud S, Merchant Z, Somavarapu S, Renshaw D. Ascorbyl palmitate/DSPE-PEG nanocarriers for oral iron delivery: preparation, characterisation and in vitro evaluation. *Colloids Surf B Biointerfaces*. 2014;115:86–92.
31. Li X, Chen D, Le C, et al. Novel mucus-penetrating liposomes as a potential oral drug delivery system: preparation, in vitro characterization, and enhanced cellular uptake. *Int J Nanomedicine*. 2011;6:3151–3162.
32. Le Tien C, Lacroix M, Ispas-Szabo P, Mateescu MA. N-acylated chitosan: hydrophobic matrices for controlled drug release. *J Control Release*. 2003;93(1):1–13.
33. Huang Y, Yu H, Guo L, Huang Q. Structure and self-assembly properties of a new chitosan-based amphiphile. *J Phys Chem B*. 2010;114(23):7719–7726.
34. Liao S-K, Hung C-C, Lin M-F. A kinetic study of thermal degradations of chitosan/polycaprolactam blends. *Macromol Res*. 2004;12(5):466–473.
35. Choi CY, Kim SB, Pak PK, Yoo D, Chung YS. Effect of N-acylation on structure and properties of chitosan fibers. *Carbohydr Polym*. 2007;68(1):122–127.
36. Zong Z, Kimura Y, Takahashi M, Yamane H. Characterization of chemical and solid state structures of acylated chitosans. *Polymer*. 2000;41(3):899–906.
37. Yun S, Habicht JP, Miller DD, Glahn RP. An in vitro digestion/Caco-2 cell culture system accurately predicts the effects of ascorbic acid and polyphenolic compounds on iron bioavailability in humans. *J Nutr*. 2004;134(10):2717–2721.
38. Zhu L, Glahn RP, Yeung CK, Miller DD. Iron uptake by Caco-2 cells from NaFeEDTA and FeSO4: effects of ascorbic acid, pH, and a Fe(II) chelating agent. *J Agric Food Chem*. 2006;54(20):7924–7928.
39. Fairweather-Tait S, Phillips I, Wortley G, Harvey L, Glahn R. The use of solubility, dialyzability, and Caco-2 cell methods to predict iron bioavailability. *Int J Vitam Nutr Res*. 2007;77(3):158–165.
40. Sinha VR, Singla AK, Wadhawan S, et al. Chitosan microspheres as a potential carrier for drugs. *Int J Pharm*. 2004;274(1–2):1–33.
41. Park JH, Cho YW, Chung H, Kwon IC, Jeong SY. Synthesis and characterization of sugar-bearing chitosan derivatives: aqueous solubility and biodegradability. *Biomacromolecules*. 2003;4(4):1087–1091.
42. Nam HY, Kwon SM, Chung H, et al. Cellular uptake mechanism and intracellular fate of hydrophobically modified glycol chitosan nanoparticles. *J Control Release*. 2009;135(3):259–267.
43. Kim JH, Kim YS, Kim S, et al. Hydrophobically modified glycol chitosan nanoparticles as carriers for paclitaxel. *J Control Release*. 2006;111(1–2):228–234.
44. Guo J, Ping Q, Jiang G, Huang L, Tong Y. Chitosan-coated liposomes: characterization and interaction with leuprolide. *Int J Pharm*. 2003;260(2):167–173.
45. Kulkarni SB, Betageri GV, Singh M. Factors affecting microencapsulation of drugs in liposomes. *J Microencapsul*. 1995;12(3):229–246.
46. Kirby CJ, Brooker BE, Law BA. Accelerated ripening of cheese using liposome-encapsulated enzyme. *Int J Food Sci Technol*. 1987;22(4):355–375.
47. Grit M, Crommelin DJ. Chemical stability of liposomes: implications for their physical stability. *Chem Phys Lipids*. 1993;64(1–3):3–18.
48. Parasassi T, Giusti AM, Raimondi M, et al. Cholesterol protects the phospholipid bilayer from oxidative damage. *Free Radic Biol Med*. 1995;19(4):511–516.
49. Samuni AM, Lipman A, Barenholz Y. Damage to liposomal lipids: protection by antioxidants and cholesterol-mediated dehydration. *Chem Phys Lipids*. 2000;105(2):121–134.
50. Ramasamy T, Haidar ZS, Tran TH, et al. Layer-by-layer assembly of liposomal nanoparticles with PEGylated polyelectrolytes enhances systemic delivery of multiple anticancer drugs. *Acta Biomater*. 2014;10(12):5116–5127.
51. Zaru M, Manca ML, Fadda AM, Antimisiaris SG. Chitosan-coated liposomes for delivery to lungs by nebulisation. *Colloids Surf B Biointerfaces*. 2009;71(1):88–95.
52. Phetdee M, Polnok A, Viyoch J. Development of chitosan-coated liposomes for sustained delivery of tamarind fruit pulp's extract to the skin. *Int J Cosmet Sci*. 2008;30(4):285–295.
53. Thongborisute J, Tsuruta A, Kawabata Y, Takeuchi H. The effect of particle structure of chitosan-coated liposomes and type of chitosan on oral delivery of calcitonin. *J Drug Target*. 2006;14(3):147–154.
54. Quemeneur F, Rinaudo M, Pépin-Donat B. Influence of molecular weight and pH on adsorption of chitosan at the surface of large and giant vesicles. *Biomacromolecules*. 2008;9(1):396–402.
55. Bhatia SC, Ravi N. A Mössbauer Study of the interaction of chitosan and d-glucosamine with iron and its relevance to other metalloenzymes. *Biomacromolecules*. 2003;4(3):723–727.
56. Dimitrova MN, Tsekov R, Matsumura H, Furusawa K. Size dependence of protein-induced flocculation of phosphatidylcholine liposomes. *J Colloid Interface Sci*. 2000;226(1):44–50.
57. Florence AT. Issues in oral nanoparticle drug carrier uptake and targeting. *J Drug Target*. 2004;12(2):65–70.
58. Heurtault B, Saulnier P, Pech B, Proust JE, Benoit JP. Physico-chemical stability of colloidal lipid particles. *Biomaterials*. 2003;24(23):4283–4300.
59. Takeuchi H, Matsui Y, Yamamoto H, Kawashima Y. Mucoadhesive properties of carbopol or chitosan-coated liposomes and their effectiveness in the oral administration of calcitonin to rats. *J Control Release*. 2003;86(2–3):235–242.
60. Lehr C-M, Bouwstra JA, Schacht EH, Junginger HE. In vitro evaluation of mucoadhesive properties of chitosan and some other natural polymers. *Int J Pharm*. 1992;78(1–3):43–48.
61. Garrick MD, Garrick LM. Cellular iron transport. *Biochim Biophys Acta*. 2009;1790(5):309–325.
62. Desai MP, Labhasetwar V, Amidon GL, Levy RJ. Gastrointestinal uptake of biodegradable microparticles: effect of particle size. *Pharm Res*. 1996;13(12):1838–1845.
63. Muthu MS, Kulkarni SA, Xiong J, Feng SS. Vitamin E TPGS coated liposomes enhanced cellular uptake and cytotoxicity of docetaxel in brain cancer cells. *Int J Pharm*. 2011;421(2):332–340.
64. Luo Y, Teng Z, Wang TT, Wang Q. Cellular uptake and transport of zein nanoparticles: effects of sodium caseinate. *J Agric Food Chem*. 2013;61(31):7621–7629.
65. Win KY, Feng SS. Effects of particle size and surface coating on cellular uptake of polymeric nanoparticles for oral delivery of anticancer drugs. *Biomaterials*. 2005;26(15):2713–2722.
66. Pappenheimer JR, Dahl CE, Karnovsky ML, Maggio JE. Intestinal absorption and excretion of octapeptides composed of D amino acids. *Proc Natl Acad Sci U S A*. 1994;91(5):1942–1945.
67. Snoeck V, Goddeeris B, Cox E. The role of enterocytes in the intestinal barrier function and antigen uptake. *Microbes Infect*. 2005;7(7–8):997–1004.